# Utilization of multiple graphene layers in fuel cells. 1. An improved technique for the exfoliation of graphene-based nanosheets from graphite

Burcu Saner, Firuze Okyay, Yuda Yürüm *

*Faculty of Engineering and Natural Sciences, Sabanci University, Orhanli, Tuzla, Istanbul 34956, Turkey*

ARTICLE INFO

*Article history:*
Received 1 June 2009
Received in revised form 22 March 2010
Accepted 23 March 2010
Available online 1 April 2010

*Keywords:*
Graphite
Graphite oxide
Graphene-based nanosheets
Exfoliation

ABSTRACT

An improved, safer and mild method was proposed for the exfoliation of graphene like sheets from graphite to be used in fuel cells. The major aim in the proposed method is to reduce the number of layers in the graphite material and to produce large quantities of graphene bundles to be used as catalyst support in polymer electrolyte membrane fuel cells. Graphite oxide was prepared using potassium dichromate/sulfuric acid as oxidant and acetic anhydride as intercalating agent. The oxidation process seemed to create expanded and leafy structures of graphite oxide layers. Heat treatment of samples led to the thermal decomposition of acetic anhydride into carbondioxide and water vapor which further swelled the layered graphitic structure. Sonication of graphite oxide samples created more separated structures. Morphology of the sonicated graphite oxide samples exhibited expanded the layer structures and formed some tulle-like translucent and crumpled graphite oxide sheets. The mild procedure applied was capable of reducing the average number of graphene sheets from 86 in the raw graphite to nine in graphene-based nanosheets. Raman spectroscopy analysis showed the significant reduction in size of the in-plane $sp^2$ domains of graphene nanosheets obtained after the reduction of graphite oxide.

## 1. Introduction

Graphite is a layered material and form by a number of two dimensional graphene crystals weakly coupled together. Graphene, the world's thinnest sheet – only a single atom thick – has a great potential to provide a new way in energy, computing and medical research [1]. It is the flat monolayer of carbon atoms in $sp^2$ hybridization. The novel structure of graphene is the center stage for all the calculations on graphite, carbon nanotubes and fullerenes. The first graphene sheets were obtained by extracting monolayer sheets from the three-dimensional graphite using a technique called micromechanical cleavage in 2004 [2].

There are many attempts in the literature for the treatment of graphite and production of monolayer graphene sheets. The first work was conducted by Brodie in 1859 and graphite oxide (GO) was prepared by repeated treatment of Ceylon graphite with an oxidation mixture consisting of potassium chlorate and fuming nitric acid [3]. Then, Staudenmaier produced GO by the oxidation of graphite in concentrated sulfuric acid and nitric acid with potassium chlorate [4]. However, this method was time consuming and hazardous. Hummers and Offeman found a rapid and safer method for the preparation of GO and in this method graphite was oxidized in water free mixture of sulfuric acid, sodium nitrate and potassium permanganate [5]. The structure of GO resembles graphite but only difference is that the $sp^3$ hybridization in carbon atoms indicates that the individual layers are considerably bent [6]. GO directly exfoliated in water due to its hydrophilic property [7].

Graphene oxide nanoplatelets can be produced via the chemical reduction of exfoliated graphite oxide in order to be used in various engineering fields due to their extraordinary mechanical, structural, thermal and electrical properties as graphite [8]. Graphene nanosheets have been obtained by the reduction of GO which was prepared by immersing graphite flakes into a mixture of concentrated sulfuric acid and nitric acid [9].

Catalyst has a crucial effect on both the cost and durability of polymer electrolyte membrane fuel cells (PEMFC). Graphene can be a promising candidate as catalyst support material for PEMFC due to its outstanding mechanical, structural, and electronic properties. Herein, the support material becomes significant to get high catalytic performance of catalysts by lower catalyst loadings [10]. The incorporation of metals into the graphene layers can be a bright opportunity to ensure thermal and electronic conductivities of the membrane electrolyte for the use as catalyst support in PEMFCs.

In the present work, we present an improved, safer and mild method for the exfoliation of graphene like sheets from graphite to be used in fuel cells. The major aim in the proposed method is to reduce the number of layers in the graphite material and to produce large quantities of graphene bundles to be used as catalyst support in PEMFCs.

* Corresponding author. Tel.: +90 216 4839512; fax: +90 216 4839550.
*E-mail address:* yyurum@sabanciuniv.edu (Y. Yürüm).

## 2. Experimental

### 2.1. Raw materials

Graphite flake (Sigma–Aldrich); acetic anhydride (Merck, extra pure); sulfuric acid (Fluka, 95–97%); potassium dichromate (Chempur, 99.9%); hydroquinone (Acros, 99%); sodium hydroxide (Merck, 97%).

### 2.2. Preparation of GO

GO was prepared according to the following method by using potassium dichromate as oxidant [11]. Using $KMnO_4$ as oxidizing agent as used in other papers was thought to be very severe and there were risks of explosions when it is used together with $H_2SO_4$. Therefore, we used a milder oxidant, $K_2Cr_2O_7$ to prevent such experimental dangers. Potassium dichromate and sulfuric acid were stirred in a flask in two different weight ratios as 0.6:6.2 and 2.1:55. For the second set, 1.5 ml distilled water was also added to prepare chromic acid. In both cases, flake graphite (1.0 g) was added to flask and the mixture was stirred gently. Then acetic anhydride (1.0 g) used as an intercalating agent was slowly dropped into the solution. The solution was stirred at 45 °C for 50 min. GO obtained was filtered and neutralized with 0.1 M NaOH and washed with distilled water until washings were neutral. After washing, GO was dried in a vacuum oven at 60 °C overnight. Experimental conditions for graphite oxidation are summarized in Table 1.

GO was exfoliated into dispersed GO sheets in distilled water for 1 h at room temperature via ultrasonic vibration.

### 2.3. Expansion of GO

GO was expanded by heating up to 900 °C rapidly in a tube furnace and kept for 15 min at this temperature under an argon atmosphere. GO samples were also expanded at 1000 °C and for 5 min. Expanded GO was subjected to ultrasonic water bath for 1 h for dispersion and then dried at 60 °C in a vacuum oven overnight.

### 2.4. Reduction of GO and expanded GO samples into graphene-based nanosheets

Expanded GO sample was exfoliated and reduced by refluxing in hydroquinone and distilled water under a $N_2$ atmosphere for 1 day. The graphene-based sheets were separated by filtration and washed with methanol and water three times and, dried in a vacuum oven at 60 °C overnight. On the other hand, unexpanded GO samples were also chemically reduced to graphene-based nanosheets by following the same reduction procedure.

### 2.5. Structural and morphological characterization

All the products obtained at different steps of the above method were investigated by a Leo Supra 35VP Field Emission Scanning Electron Microscope (SEM). X-ray diffraction (XRD) measurements were done with a Bruker AXS advance powder diffractometer fitted with a Siemens X-ray gun, using Cu $K_\alpha$ radiation ($\lambda$ = 1.5406 Å). The samples were rotated at 10 rpm and swept from $2\theta = 10°$ through to 90° using default parameters of the program of the diffractometer that was equipped with Bruker AXS Diffrac PLUS software. The X-ray generator was set to 40 kV at 40 mA. The numbers of the layers of the samples were calculated by using the classical Debye–Scherrer equations:

$$t = 0.89\lambda/\beta_{002}\cos\theta_{002}$$
$$n = t/d_{002}$$

where $t$ is the thickness; $\beta$ is the full width at half maximum (FWHM); $n$ is the number of graphene layers; $d_{002}$ interlayer spacing.

Structural changes were examined by Renishaw InVia Reflex Raman Microscopy System using (Renishaw Plc., New Mills, Wotton-under-Edge Gloucestershire, UK) using a 514 nm argon ion laser in the range of 100–3200 $cm^{-1}$.

**Table 1**
Experimental conditions for graphite oxidation.

| Experiment # | Graphite flake (g) | Acetic anhydride (g) | Concentrated sulfuric acid (g) | Potassium dichromate (g) |
|---|---|---|---|---|
| 1 | 1 | 1 | 6.2 | 0.6 |
| 2 | 1 | 1 | 55 | 2.1 |

## 3. Results and discussion

### 3.1. Graphite oxide, GO

SEM image of the raw natural graphite contained sharp, rigid and compacted layers, Fig. 1. Effect of amount of acid used in the oxidation reactions on the morphology of GO prepared was investigated also by SEM. The graphite oxide sheets became swollen, after the treatment of graphite flakes according to the 1st experimental conditions (Table 1), Fig. 2. The oxidation process seemed to create expanded and leafy structures of graphite oxide layers. SEM images of graphite samples treated according to the 2nd experimental conditions (Table 1) indicated that the layers were further swollen when using higher amount of sulfuric acid in the oxidation experiment, Fig. 3. It appeared that higher sulfuric acid amount increased the effect of oxidation caused by the dichromate ions. With this amplified effect of oxidation, it was possible that more oxygen atoms were force to attach to graphite layers which resulted in a more loose structure compared to that of the rigid structure of raw graphite.

Sonication of GO samples created more separated structures. Morphology of the sonicated GO samples exhibited expanded the layer structures and formed some tulle-like translucent and crumpled graphite oxide sheets as presented by the SEM image in Fig. 4.

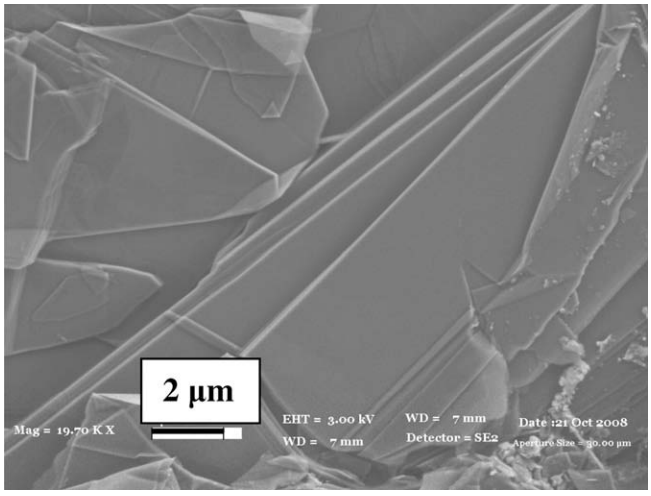


**Fig. 1.** SEM image of raw graphite flake.

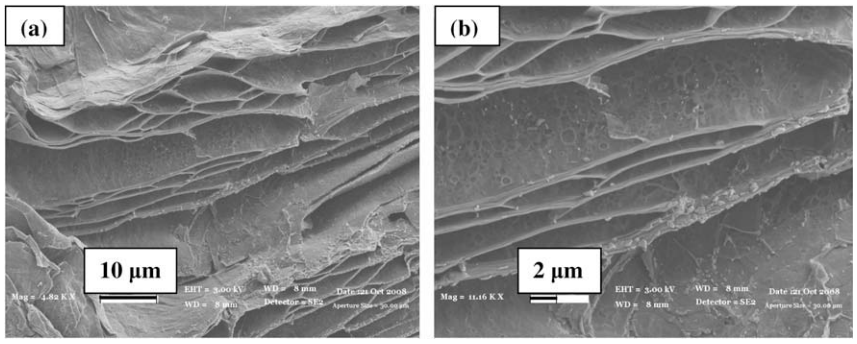


**Fig. 2.** SEM images (a) and (b) of GO at different sites. Graphite oxidation was conducted according to 1st experimental conditions in Table 1.

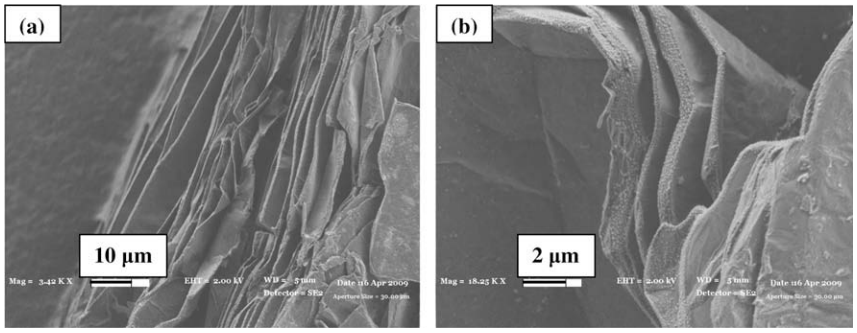


**Fig. 3.** SEM images (a) and (b) of GO at different sites. Graphite oxidation was conducted according to 2nd experimental conditions in Table 1.

### 3.2. Expanded GO

Potassium dichromate oxidation of the raw graphite created oxygenated polar structures on the surface of graphite layers after the cleavage of C–C bonds which facilitated the diffusion of acetic anhydride and oxygen into the layers. The oxidation step depends on the amount of sulfuric acid used in this reaction [11]. Heat treatment of such treated samples led to the thermal decomposition of acetic anhydride into $CO_2$ and $H_2O$ vapor which further swelled the layered graphitic structure. SEM images of the GO samples (prepared regarding to 1st experiment in Table 1) that expanded during heating under an argon atmosphere at 900 °C for 15 min in a tube furnace are presented in Fig. 5a and b. The heat treatment process caused the expansion of graphitic crystal lattice, and further separated the tulle-like GO sheets as it was the case after the sonication step. The tulle-like GO sheets were even more easily observable after the 15 min-heat treatment. GO samples obtained after 2nd experiment (Table 1) were also expanded at 1000 °C for 5 min and the layers became wavy but the tulle-like layers of this sample could not be easily observed, Fig. 6a and b. This might have stemmed from the short of heat treatment period that could not initiate the separation of the tulle-like GO sheets.

Sonications of thermally expanded GO samples produced smoother and wider tulle-like GO sheets, Fig. 7a and b. Some unexfoliated graphitic layers were observable through semi-transparent GO sheets separated in this work, Fig. 7a.

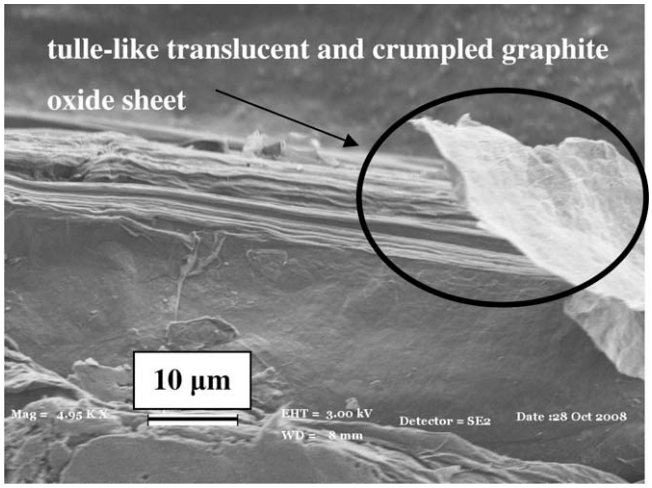


**Fig. 4.** SEM image of GO (oxidation process using 1st experimental conditions in Table 1) after sonication for 1 h at room temperature.

### 3.3. Chemical reduction of GO sheets

GO and expanded GO samples were chemically reduced by refluxing with hydroquinone in water in order to obtain graphene-based nanoplatelets. During this reaction, it is known that hydroquinone loses either one $H^+$ ion from one of its hydroxyls to form a monophenolate ion or two $H^+$ ions from both hydroxyls to form a diphenolate ion called as quinone [12]. Reflux solution became yellowish during reduction by hydroquinone. The solid product was separated by filtration at the end of the experiment, washed with water, methanol and dried.

SEM images of graphene-based nanosheets obtained after the chemical reduction experiment are presented in Fig. 8. Ruffled appearance of tulle-like graphene-based sheets was very easily observable in these images. Investigation of all regions of the reduced samples by SEM revealed that the experimental procedure was successful and yielded exfoliated graphene-based sheets.

### 3.4. Structural analysis by XRD

XRD patterns of raw graphite, GO, expanded GO and graphene-based nanosheets are presented in Figs. 9–12. The XRD pattern of

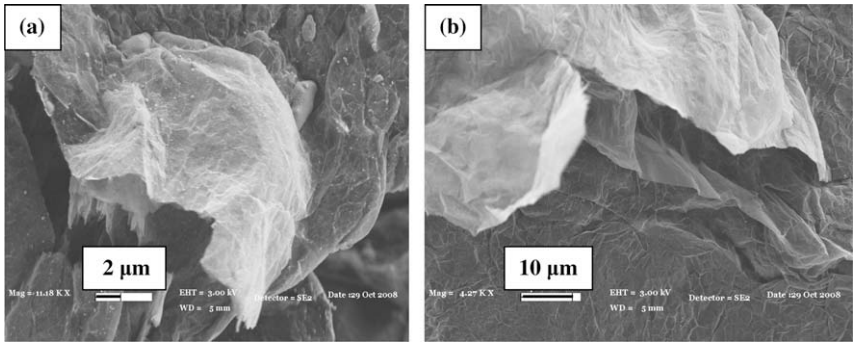


**Fig. 5.** SEM images (a) and (b) of expanded GO obtained at 900 °C for 15 min expansion.

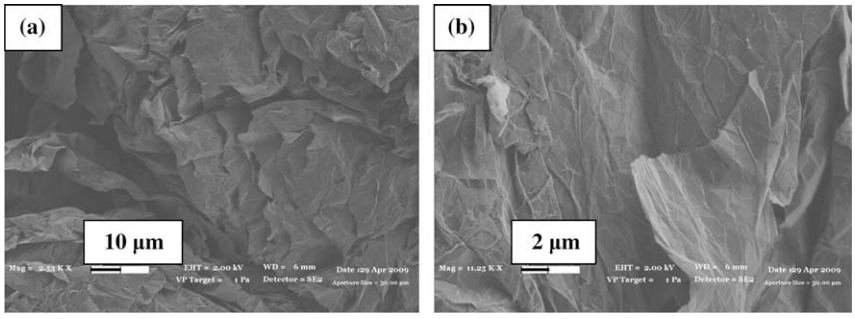


**Fig. 6.** SEM images of (a) and (b) of expanded GO obtained at 1000 °C for 5 min expansion.

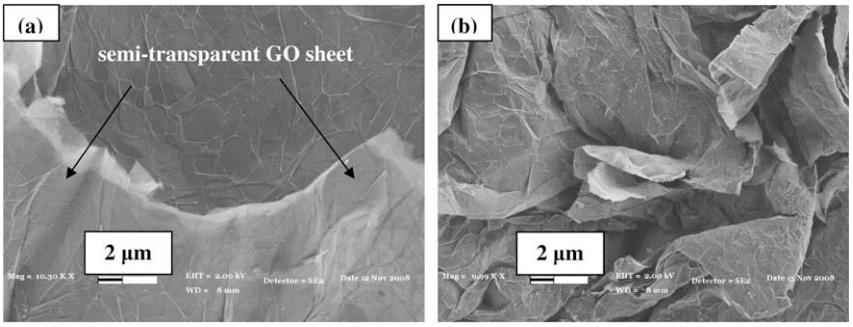


**Fig. 7.** SEM images (a) and (b) of expanded GO (prepared using 1st experimental conditions in Table 1) obtained at 900 °C for 15 min expansion after sonication for 1 h at room temperature.

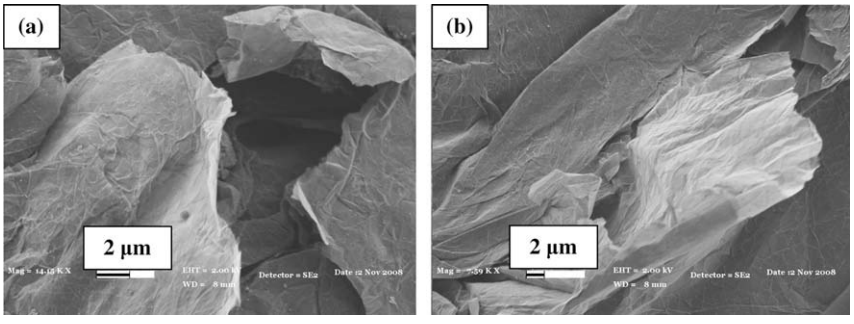


**Fig. 8.** SEM images of graphene like nanosheets obtained from different regions of the sample.

raw graphite sample contained a very sharp and high intensity 002 peak near $2\theta = 26.5°$ and 004 peak near $2\theta = 54.5°$ (Fig. 9). XRD pattern of GO which was obtained by using 1st oxidation conditions in Table 1 (Fig. 10a) contained a wide peak at $2\theta = 25.7°$ and a shoulder at near $2\theta = 28.8°$. Jihui-Li et. al. [13] also observed a similar diffraction pattern and a shoulder at 28° in the X-ray diffraction

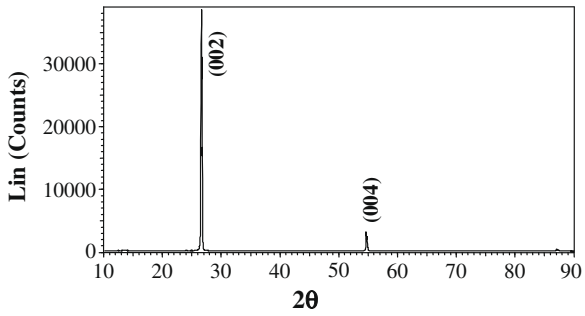


**Fig. 9.** XRD pattern of raw graphite.

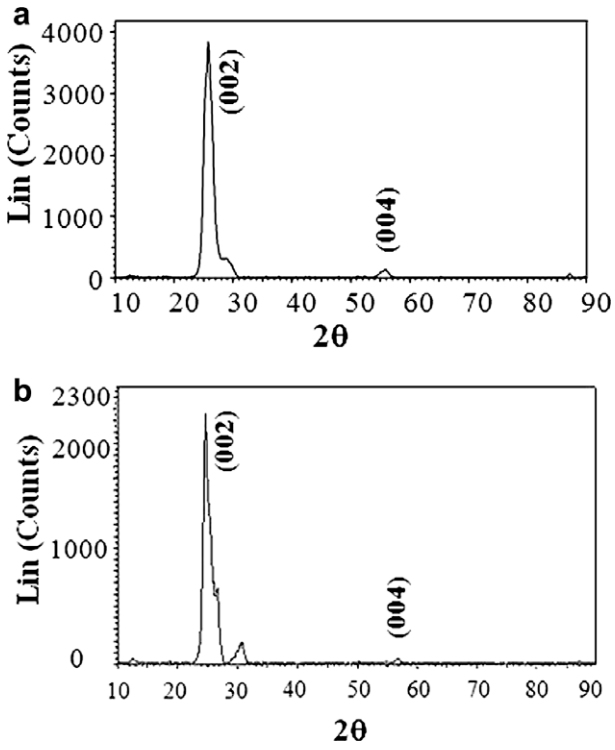


**Fig. 10.** XRD patterns of (a) GO (Oxidation process was conducted by using 1st experimental condition in Table 1) and (b) GO (oxidation process was conducted by using 2nd experimental condition in Table 1).

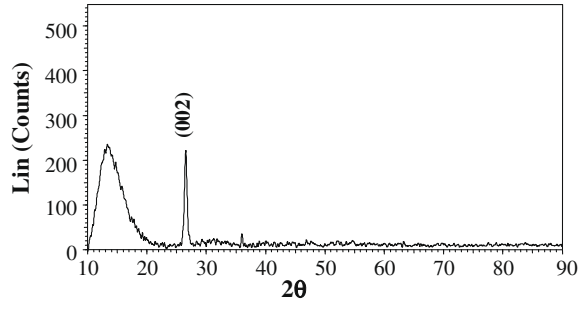


**Fig. 11.** XRD pattern of expanded GO obtained at 900 °C for 15 min expansion.

pattern for graphite intercalated compound (GIC). The reason that this shoulder was observed at 28° was due to the intercalating agent used in the present work as it was also in the work of Jihui-Li et. al. [13]. Also, XRD pattern of GO which was obtained by

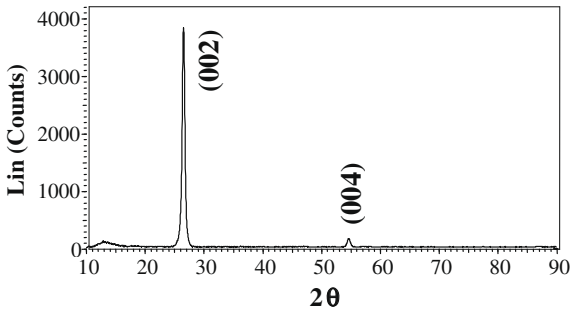


**Fig. 12.** XRD pattern of the graphene-based nanosheets after chemical reduction of expanded GO.

using 2nd oxidation conditions in Table 1 contained a sharper and shifted shoulder at around $2\theta = 30°$ (Fig. 10b) likely due to increase in the amount of oxidant between the layers.

Due to oxidation, the crystal nature of the raw graphite was changed and occurrence of a broad 001 peak near $2\theta = 14°$, and a relatively wider and very low intensity 002 peak near $2\theta = 27.5°$ were observed in the XRD pattern of expanded GO (Fig. 11). Chemical reduction restored the crystal structure again in graphene-based nanosheets by removing the effect of oxidation observed in the expanded GO sample; a sharp and high intensity 002 peak near $2\theta = 26.5°$ was observed in the XRD pattern of the graphene-based nanosheets and the 001 peak near $2\theta = 13–14°$ owing to oxidation of graphite was barely detected in the diffractrogram (Fig. 12).

Average numbers of graphene layers calculated using the Debye–Scherrer equation are presented in Tables 2 and 3. Debye–Scherrer equation was also used previously by Sakintuna and Yurum [14] in the X-ray diffraction analysis of crystallites produced during the carbonization of Turkish lignite. Gurudatt and Tripathi [15] claimed that stacking height and lateral size of the crystallites calculated by Debye–Scherrer equation were not actually equal to the exact height and size but in fact gave convenient relative estimates of actual stacking height and lateral size of the crystallites produced in the carbonization and this can also be assumed correct for the graphene structures. The graphene structures produced in the present work were not flat and therefore the values obtained by Debye–Scherrer equation were reasonable estimates that described the situation.

**Table 2**
Number of layers and interplanar spacing ($d$) of samples from XRD characterization results (oxidation process using 1st experimental conditions in Table 1).

| Samples | Average number of layers | $d$ (Å) |
|---|---|---|
| Raw graphite | 86 | 3.37 |
| GO | 14 | 3.46 |
| Expanded GO | 56 | 3.36 |
| Graphene-based nanosheets | 44 | 3.39 |

**Table 3**
Effect of sonication on the number of layers and interplanar spacings ($d$) of samples from XRD characterization results (oxidation process using 2nd experimental conditions in Table 1).

| Samples | Average number of layers | $d$ (Å) |
|---|---|---|
| Graphite flake | 86 | 3.37 |
| Sonicated graphite flake | 79 | 3.35 |
| GO | 17 | 3.61 |
| Sonicated GO | 12 | 3.64 |
| Graphene-based nanosheets | 9 | 3.62 |

Average number of layers calculated for raw graphite, GO, expanded GO and graphene-based nanosheet samples were 86, 14, 56, and 44, respectively (Table 2). The increase of layer numbers from 14 to 56 after the expansion process was the result of stacking of the layers due to the removal of acetic anhydride group that intercalated the graphene planes and the decrease in interplanar spacing (near to pristine graphite value). Sonication process was not applied to these samples to discriminate the effect of dispersion on the layer numbers. On the other hand, the average number of layers for raw graphite, sonicated graphite, GO, sonicated GO and graphene-based nanosheets were calculated as 86, 79, 17, 12 and 9 (Table 3). The stepwise chemical procedure used in the present report indicated that the average number of graphene layers reduced steadily from raw graphite to graphene nanosheet samples. Change of interplanar spacings also explained how each step in the proposed procedure affected the morphology of graphite. In the oxidation step, the interplanar spacing increased by the introduction of oxygen groups between the graphene layers in raw graphite. Sonication process after each step decreased the number of layers. The mild procedure applied was capable of reducing the average number of graphene sheets from 86 in the raw graphite to 9 in graphene-based nanosheets. When comparing the values in Tables 2 and 3, results indicated that the expansion step in the procedure has potential drawback due to the increase of the layer number in graphitic structure. Application of more severe chemical methods might reduce the number of graphene layers further.

### 3.5. Raman spectroscopy characterization

Raman spectroscopy is a quick and accurate technique to determine the number of graphene layers and the change of crystal structure of the materials after chemical treatments [16]. There are four remarkable peaks in the Raman spectrum of graphite which are the G line around 1580 $cm^{-1}$, the G′ line (the overtone of the G line) around 3248 $cm^{-1}$, the D line around 1360 $cm^{-1}$ and the D′ line (the overtone of the D line) around 2700 $cm^{-1}$. The intensity of the D line depends on the amount of the disorderness of the graphitic materials and its position shifts regarding to incident laser excitation energies [16]. A strong G line at 1580 $cm^{-1}$, a weak D line at 1360 $cm^{-1}$ and a broad D′ line at 2724 $cm^{-1}$ were seen in the Raman spectrum of raw graphite, Fig. 13. After oxidation process, G line of GO sample was broadened and the intensity of D line was increased due to the reduction in the thickness of the graphitic structure, Fig. 14. In the Raman spectrum of reduced GO, the G line was broadened and shifted to 1600 $cm^{-1}$, Fig. 15. In addition, an increased intensity of the D line around 1355 $cm^{-1}$ indicated the considerable reduction in size of the in-plane $sp^2$ domains owing to oxidation and sonication processes, and the formation of graphene nanosheets having highly oriented crystal structure. In the Raman spectrum of graphene-based nanosheets obtained after chemical reduction of expanded GO, the intensity of the D line around 1356 $cm^{-1}$ decreased considerably as a result of an increase of the graphitic domain sizes and an increase of the thickness of graphitic structure after thermal treatment, Fig. 16. This increase could also be seen by the increase in the number of average graphene layers after thermal treatment that was calculated from X-ray diffraction patterns by using Debye–Scherrer equation as observed in Table 3.

For the comparison of the structural changes after the chemical treatments, another critical factor was the disorder amount. As the structure changes from graphite to nanocrystalline graphite, the ratio between the intensity of D and G line, $I(D)/I(G)$, changes inversely with the size of the crystalline grains or interdefect distance [17]. $I(D)/I(G)$ values for graphite, GO, reduced GO and

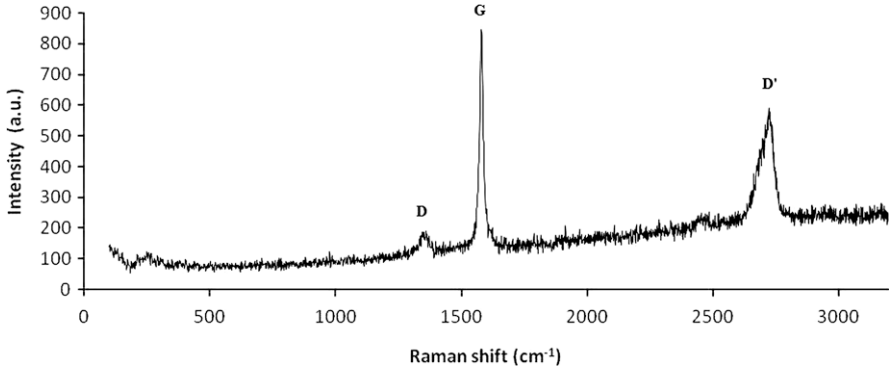


**Fig. 13.** Raman spectrum of raw graphite.

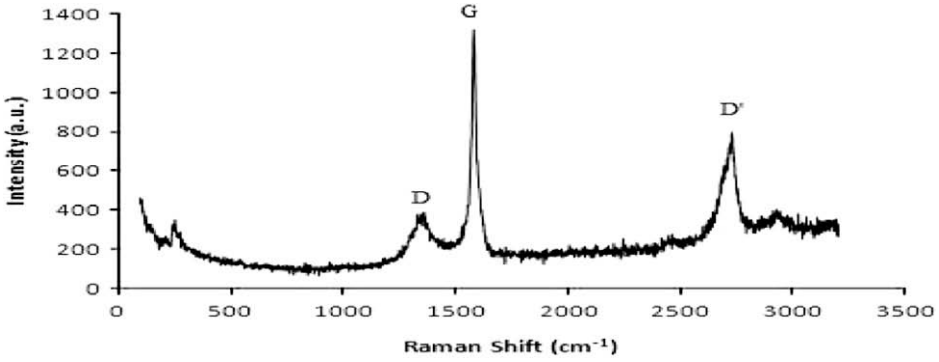


**Fig. 14.** Raman spectrum of GO.

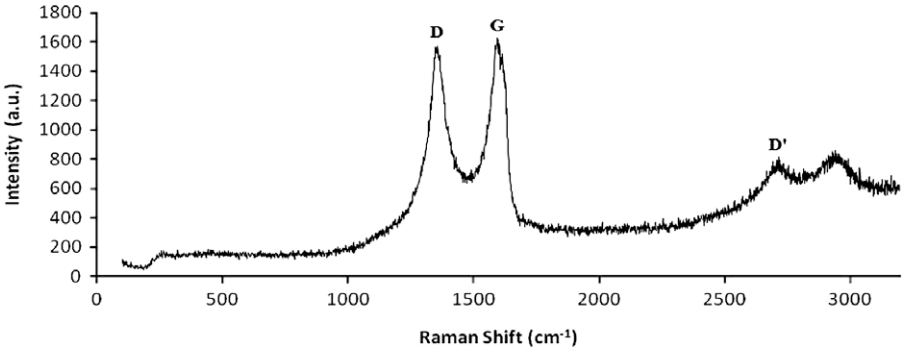


**Fig. 15.** Raman spectrum of graphene-based nanosheets after chemical reduction of GO.

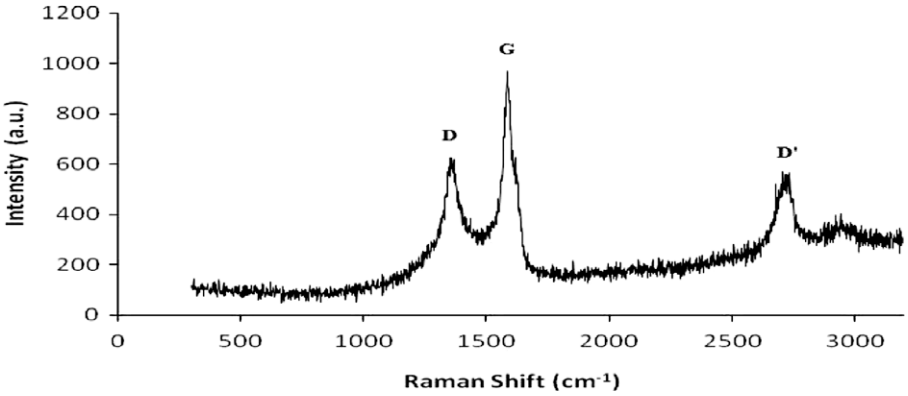


**Fig. 16.** Raman spectrum of graphene-based nanosheets after chemical reduction of expanded GO.

reduced expanded GO were calculated as 0.2, 0.3, 1.0 and 0.6, respectively. The highest $I(D)/I(G)$ ratio of reduced GO sample was evidence for the structure with highest order.

When the layer number is smaller than five, the D′ peak becomes more intense than G peak [18]. The increase in the ratio between the intensity of G and D' peak, $I(G)/I(D')$, indicated an increase in the number of graphene layers. $I(G)/I(D')$ values for graphite, GO, reduced GO and reduced expanded GO were estimated as 1.5, 1.6, 2.1 and 1.8, respectively. The highest $I(G)/I(D')$ ratio of reduced GO sample demonstrated the largest number of graphene layers.

## 4. Conclusions

Graphene like nanosheets to be used as catalyst support material in PEMFC applications were obtained in moderate quantities by improved, safer and mild chemical route applied in the present work. With the chemical procedure used, GO was prepared by using concentrated sulfuric acid, acetic anhydride and potassium dichromate from raw graphite. The steps of thermal expansion, ultrasonic treatment and chemical reduction process yielded graphene like nanosheets. The best method for the production of mostly exfoliated (minimum number of layers) graphene nanosheets is the oxidation of the sonicated graphite flake, ultrasonic treatment of GO, and chemical reduction of sonicated GO samples. Thermal expansion process should be eliminated in the procedure because this step led to stack the layers in graphitic structure and increase the layer numbers of graphene nanosheets. The results from each step were investigated in details by SEM, XRD and Raman spectroscopy. SEM images exhibited that graphene like layers can exist by being rippled rather than completely flat in a free standing state. The XRD results put forward that the number of graphene sheets decreased in each step from 86 (raw graphite) to nine (reduced GO). The analysis of structural changes from raw graphite to graphene nanosheets in Raman spectra displayed the significant reduction of the graphitic domain sizes after the reduction of GO. The effective surface area of graphene sheets as catalyst support material relies on the layer numbers. When the layer number in graphitic structure decreases, the effective surface area increase and thus increase the metal-support interaction. Consequently, durability of the catalyst on graphene-based catalyst support increases and this causes better fuel cell performance. Work still continues to enhance the technique for the production of individual graphene sheets.

## References

[1] Stoller MD, Park S, Zhu Y, An J, Ruoff RS. Graphene-based ultracapacitors. Nano Lett 2008;8:3498–502.
[2] Novoselov KS, Geim AK, Morozov SV, Jiang D, Zhang Y, Dubonos SV, et al. Electric field effect in atomically thin carbon films. Science 2004;306:666.
[3] Brodie BC. On the atomic weight of graphite. Philos Trans R Soc London 1859;149:249.
[4] Staudenmaier L. Verfahren zur darstellung der graphitsaure. Ber Dtsch Chem Ges 1898;31:1481.
[5] Hummers WS, Offeman RE. Preparation of graphitic oxide. J Am Chem Soc 1958;80:1339.
[6] Karpenko GA, Turov VV, Kovtyukhova NI, Bakai EA, Chuiko AA. Graphite oxide structure and $H_2O$ sorption capacity. Theor Exp Chem 1990;26:94.
[7] Titelman GI, Gelman V, Bron S, Khalfin RL, Cohen Y, Bianco-Peled H, et al. Characteristic and microstructure of aqueous colloid dispersions of graphite oxide. Carbon 2005;43:641.
[8] Stankovich S, Dikin D, Piner RD, Kohlhaas KA, Kleinhammes A, Jia Y, et al. Synthesis of graphene-based nanosheets via chemical reduction of exfoliated graphite oxide. Carbon 2007;45:1558.
[9] Wang G, Yang J, Park J, Gou X, Wang B, Liu H, et al. Facile synthesis and characterization of graphene nanosheets. J Phys Chem C 2008;112:8192.
[10] Shao Y, Liu J, Wang Y, Lin Y. Novel catalyst support materials for PEM fuel cells: current status and future prospects. J Mater Chem 2009;19:46–59.
[11] Li J, Feng L, Jia Z. Preparation of expanded graphite with 160 μm mesh of fine flake graphite. Mater Lett 2006;60:746–9.

[12] Jia YF, Demopoulos GP. Adsorption of silver onto activated carbon from acidic media: nitrate and sulfate media. Ind Eng Chem Res 2003;42:72.
[13] Huifang-Da, Jihui-Li, Qian-Liu, Shufen-Liu. Preparation of sulfur-free expanded graphite with 320 μm mesh of flake graphite. Mater Lett 2006;60:3927–30.
[14] Sakintuna B, Cetinkaya S, Yurum Y. Evolution of carbon microstructures during the pyrolysis of Turkish Elbistan lignite in the temperature range of 700–1000°C. Energy Fuels 2004;18:883–8.
[15] Gurudatt K, Tripathi VS. Studies on changes in morphology during carbonization and activation of pretreated viscose rayon fabrics. Carbon 1998;36:1371–7.
[16] Graf D, Molitor F, Ensslin K, Stampfer C, Jungen A, Hierold C, et al. Spatially resolved Raman spectroscopy of single- and few-layer graphene. Nano Lett 2007;7:238–42.
[17] Ferrari AC, Robertson J. Interpretation of Raman spectra of disordered and amorphous carbon. Phys Rev B 2000;61:14095–107.
[18] Gupta A, Chen G, Joshi P, Tadigadapa S, Eklund PC. Raman scattering from high-frequency phonons in supported *n*-graphene layer films. Nano Lett 2006;6:2667.